Available online at www.sciencedirect.com
ScienceDirect
Trans. Nonferrous Met. Soc. China 32(2022) 2110−2124
Transactions of Nonferrous Metals Society of China
www.tnmsc.cn

Evolution of V-containing phases during preparation of Al-based Al−V master alloys

Yi MENG[1], Yue YANG[1], Cen LI[1], Lei-gang CAO[1], Zhi-hao ZHAO[2], Qing-feng ZHU[2,3], Jian-zhong CUI[3]

1. School of Mechanical and Materials Engineering, North China University of Technology, Beijing 100144, China;
2. College of Materials Science and Engineering, Northeastern University, Shenyang 110004, China;
3. Key Lab of Electromagnetic Processing of Materials, Ministry of Education, Northeastern University, Shenyang 110004, China

Received 15 July 2021; accepted 16 December 2021

Abstract: Al-based Al−V master alloys were prepared by both the stepwise heating melting experiment and stepwise melting cooling experiment with rapid solidification to investigate the transformation of V-containing phases which gave different effects on microstructures and properties of commercial Al alloys and Ti alloys, as both melting and solidification processes affect the evolution of V-containing phases largely. The results showed that the raw Al−50wt.%V alloy consisted of needle-like Al_3V phase and Al_8V_5 phase (matrix), while petal-like Al_3V, needle-like Al_7V and plate-like $Al_{10}V$ phase were present in the Al−V master alloys. The metastable Al_7V phase was evolved from Al_3V phase and then evolved into $Al_{10}V$ phase during melting process. The number of $Al_{10}V$ phase increased with the decrease of temperature in the range of 800−1000 °C. Petal-like Al_3V phases could be transformed from Al_8V_5 phase, pre-precipitated from Al−V molten liquid during melting process and precipitated directly during rapid solidification, respectively.

Key words: Al-based Al−V master alloy; phase transformation; vanadium-containing phase; rapid solidification; pouring temperature

1 Introduction

The addition of trace elements is an effective method to improve the microstructures and mechanical properties of aluminum alloys [1,2]. One of them is vanadium element [3−8]. 0.1 wt.% V addition could improve the strength of A356 alloy at room temperature [3], but limit its high-temperature properties [4]. The formation of stable quaternary AlFeVSi phase in the as-extruded alloy with 0.1 wt.% V element enhanced the pinning effect on the dislocation movement [5]. Combined additions of Cr, Zr, Ti, and V into Al−7Si−1Cu−0.5Mg (wt.%) alloy developed a complex microstructure, which contains many V-containing phases: $Al_{13}(FeCrVTi)_4Si_4$, $(AlSi)_3$-(CrVTi), and α-$Al_{12}(FeCrV)_3Si$ [6]. The addition of 0.25 wt.% V caused the grain refinement of Al−7Si−3Cu−0.3Mg (wt.%) alloy by the formation of $(AlSi)_2(VTiMn)$ particles and V accumulation in α-$Al_{15}(FeMn)_3Si_2$ phase [7]. Moreover, $Al_3(Zr,V)$ could inhibit the grain coarsening during the isochronal aging treatments of Al−0.031Er−0.033Sc−0.236Zr−0.062Si (wt.%) alloy containing 0.15 wt.% V [8]. Therefore, V-containing phases with various characteristics, formed in the processes of production and subsequent treatments of commercial Al alloys, gave rise to different impacts on the microstructures and mechanical properties of commercial Al alloys.

In order to avoid mass loss at high temperature,

Corresponding author: Yi MENG, Tel: +86-10-88802105, E-mail: mengyi@ncut.edu.cn
DOI: 10.1016/S1003-6326(22)65934-X

many trace elements, such as Ti, Sc, V and Zr, were added in the form of master alloys, instead of pure elements [1,2,9,10]. For example, the addition of Al−5wt.%Ti master alloys could cause different degree of grain refinement of commercial Al alloys according to the morphology, size and quantities of Al_3Ti phase in the master alloy [11,12]. Flaky-shaped Al_3Zr phases in Al−Zr master alloy facilitated the formation of $L1_2$ cubic structure [13−17] and DO_{23} tetragonal structure [14,15] during the subsequent treatment of commercial Al alloys.

Therefore, it could be found that the chemical formula of both Ti-containing phase and Zr-containing phase was always unique [18,19]. However, various V-phases (Al_3V and $Al_{10}V$) were formed during the preparation of Al-based Al−V master alloys [20,21], resulting in quite different effects and evolution in their subsequent adding process as well [22]. Further, LAI et al [23], and SHI and CHEN [24] found that, V addition into the 7150 aluminum alloy induced a large number of near spherical V-containing dispersoids and a few rod-like $Al_{21}V_2$ phases which were also designated as $Al_{10}V$ phase [25]. But the microstructure evolution of V-containing phases still needed to be discussed in detail, including the preparation of Al-based Al−V master alloys.

Our team previously found that V content and melting temperature determined the formation of Al_3V phase and $Al_{10}V$ phase [20], but the questions about locations where Al_3V and $Al_{10}V$ phases come from and the transformation between these two phases were still not discussed clearly. In this work, the whole processes of different V-containing phase evolution, from the raw material (Al−50wt.%V alloy) to various as-cast Al-based Al−V master alloys produced by means of stepwise heating melting experiment and stepwise melting cooling experiment at different temperatures were studied in detail.

2 Experimental

2.1 Preparation of Al-based Al−V master alloys by different methods

High purity aluminum (99.99 wt.%) and Al−50wt.%V alloy were chosen as the raw materials to fabricate Al−4wt.%V alloy. Pure aluminum ingot was firstly melted at 800 °C in a graphite crucible by using a well type resistance furnace. Al−50wt.%V fine particles were then added into the molten aluminum alloy with the assistance of mechanical stirrer to ensure chemical homogeneity. In order to study the evolution of V-containing phases with temperature, both the stepwise melting cooling experiment and stepwise heating melting experiment with rapid solidification obtained by the water-cooled copper mould were carried out to produce Al-based Al−V master alloys at different pouring temperatures. The temperature at the center of water-cooled copper mould during rapid solidification was collected by HIOKI data collector with the collecting cycle being 10 ms, which gave the way to figure out the cooling rate of the rapid solidification. The processes of both melting experiments were illustrated as follows and shown in Fig. 1.

(1) Stepwise heating melting experiment (Fig. 1(a)): The mixed molten alloy of pure aluminum and Al−50wt.%V alloy was held at 800 °C and then heated to 900, 1000, 1050, 1100

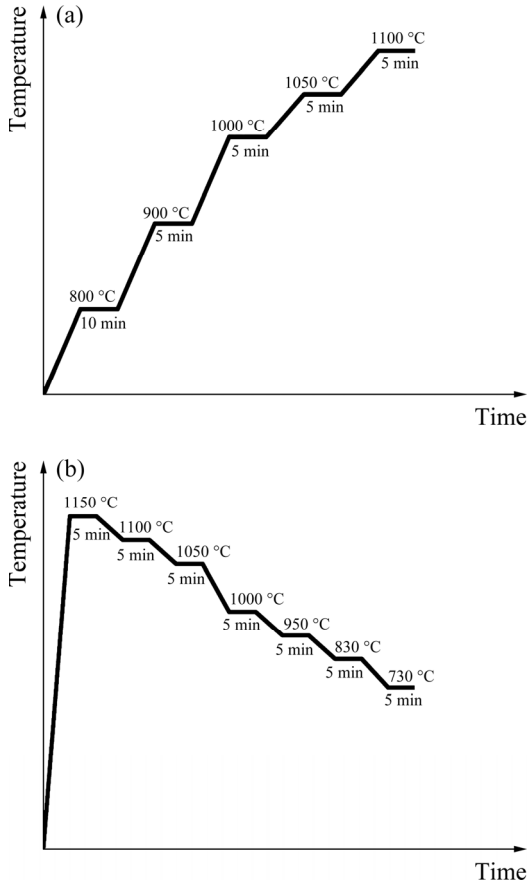

Fig. 1 Heating and cooling curves obtained by stepwise heating melting (a) and stepwise melting cooling (b) experiments

and 1150 °C step by step. At each temperature stage, the holding time of the molten alloy was 5 min and then some molten alloy was taken out and poured into the water-cooled copper mould.

(2) Stepwise melting cooling experiment (Fig. 1(b)): The mixed molten alloy was heated to 1150 °C directly with mechanical stirring at least 3 times and then dropped down to 1100, 1050, 1000, 950, 830 and 730 °C step by step. Similarly, after being held for 5 min at each temperature stage, some molten alloy was bailed out at each temperature stage and poured into the water-cooled copper mould.

2.2 Microstructure analysis and chemical composition test

Metallographic specimens were taken from the center of ingots and then electrolytically polished by using a solution of 20 vol.% $HClO_4$ and 80 vol.% ethanol at 0.7 A for 1−2 min. The microstructures were observed by using the OLYMPUS LEXT OLS4100 three-dimension (3D) laser scanning microscope. The detailed information of V-containing phases was identified by using an X-ray diffractometer (XRD), a scanning electron microscope (SEM) equipped with an energy dispersive spectrometry detector (EDS), and a transmission electron microscope (TEM). The scan range of XRD test is 5°−110° with a scanning rate of 4 (°)/min. The chemical compositions of Al-based Al−V master alloys were measured by inductively coupled plasma atomic emission spectrometry (ICP-AES).

3 Results

3.1 V-containing phases in raw Al−50wt.%V alloy

Figure 2 shows the microstructures of V-containing phases in the raw Al−50wt.%V alloy. Figures 2(a) and (b) indicate large quantities of needle-like phases, and each of them is surrounded by “black bands”. According to the 3D image shown in Fig. 2(c), it is clear that the “black bands” around the needle-like phase are caused by the protrusion of needle-like phase from the matrix, instead of another phase surrounding the needle-like phase.

Figure 3 indicates the XRD analysis result of Al−50wt.%V alloy, showing that Al−50wt.%V alloy

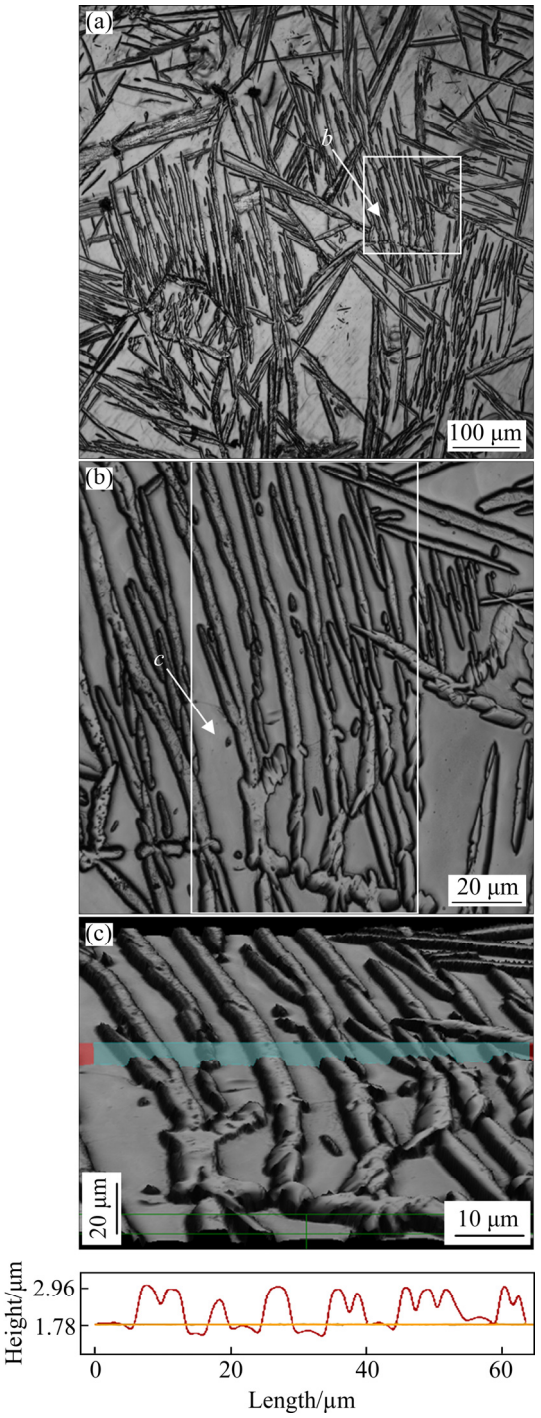

Fig. 2 Microstructures of raw Al−50wt.%V alloy by 3D measuring laser microscope: (a) Image of alloy; (b) Magnified image of Area *b* in (a); (c) 3D image of Area *c* in (b) and curve of height at corresponding position

consists of two phases: Al_8V_5 and Al_3V. Further, the elemental compositions of constituent phases of Al−50wt.%V alloy are shown in Fig. 4. The electron backscattered image (Fig. 4(a)) illustrates the random distribution of needle-like Phase B in

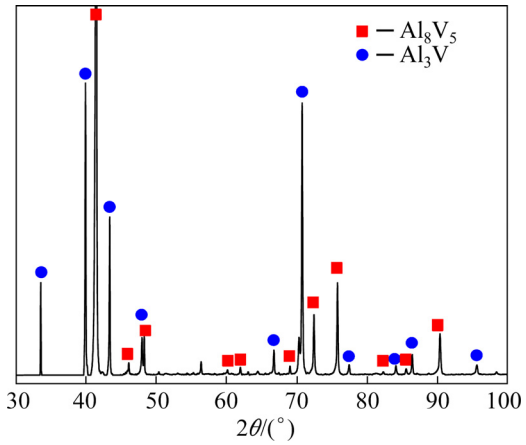

Fig. 3 XRD analysis result of Al−50wt.%V alloy

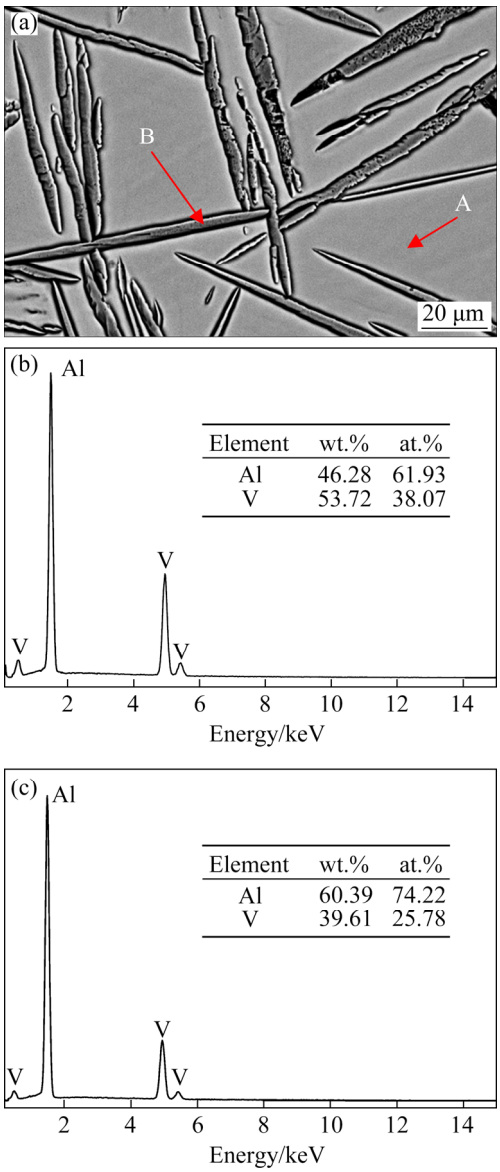

Fig. 4 SEM image and EDS analysis results of Al−50wt.%V alloy: (a) SEM image of alloy; (b) EDS analysis result of matrix (Phase A) in (a); (c) EDS analysis result of Phase B in (a)

the matrix Phase A. The elemental compositions of Phases A and B are given in Figs. 4(b) and (c), respectively, indicating that the matrix (Phase A) is Al_8V_5 phase and the needle-like Phase B is Al_3V phase.

3.2 Cooling rate in water-cooled copper mould at different pouring temperatures

Figure 5 shows the dependence of temperature on time measured by thermocouple located at the center of the water-cooled copper mould after the Al−V molten alloys were poured into the mould at temperatures (T_{melt}) of 800, 900, 1000 and 1100 °C. A significant increase in temperature can be observed in each curve at first and then the temperature drops down quickly as shown in Fig. 5(a). As the time spent on the temperature increase in all the curves is less than 3.5 s, the temperature−time behavior in the first 3.5 s of the

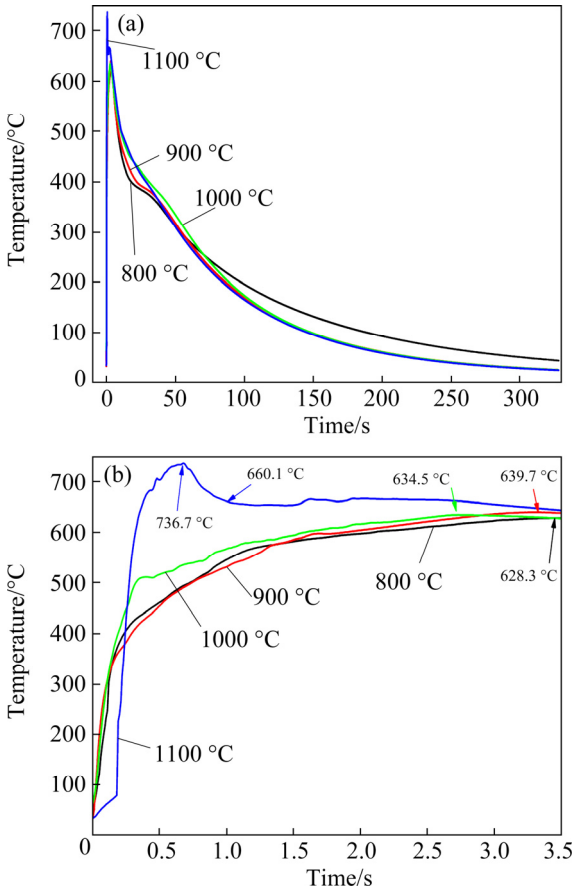

Fig. 5 Dependence of temperature at center of water-cooled copper mould measured by thermocouple on time during cooling at different pouring temperatures: (a) Whole cooling curves at corresponding pouring temperatures; (b) Magnified temperature−time curves for the first 3.5 s of curves in (a)

curves is demonstrated in Fig. 5(b). It should be acceptable that the temperature measured by thermocouple increases rapidly once the molten Al−V alloy is poured into the water-cooled copper mould from room temperature, while the temperature of molten Al−V alloy decreases dramatically at the same time in the rapid solidification process. Therefore, the maximum temperatures recorded by thermocouple are lower than the corresponding pouring temperature. As shown in Fig. 5(b), the maximum temperatures of alloys prepared at the pouring temperatures of 800, 900, 1000 and 1100 °C are measured to be 628.3, 639.7, 634.5 and 736.7 °C, respectively.

In fact, the temperature of the molten alloy keeps on decreasing from the pouring temperature in the entire rapid solidification process. Thus, the cooling rate ($v_{cooling}$) of the molten alloy from the pouring temperature (T_{melt}) to the maximum temperature (T_{max}) recorded by thermocouple can be simply estimated by Eq. (1):

$$v_{cooling}=(T_{melt}-T_{max})/t \quad (1)$$

where t is the time reaching the maximum temperature recorded by thermocouple from room temperature.

Although the alloys were poured into copper mould at 800, 900 and 1000 °C, the maximum temperatures measured by thermocouple are much lower than 660.1 °C (Fig. 5(b)). This indicates that the solidification process was completed within the first 3.5 s of the temperature−time curves based on the Al−V binary phase diagram [25,26]. So, the solidification rates for the alloys at pouring temperatures of 800, 900 and 1000 °C can be estimated to be about 49, 79 and 134 °C/s, respectively.

However, the maximum temperature of the molten alloy recorded by thermocouple at the pouring temperature of 1100 °C increases to 736.7 °C in 0.68 s, indicating the existence of the remaining liquid at this moment. So, the corresponding cooling rate within the first 0.68 s was estimated to be ~534 °C/s according to Eq. (1) and the corresponding cooling rate between 736.7 °C and 660.1 °C is ~232 °C/s.

Considering the fact that the alloys experience high cooling rate, if some V-containing phases are precipitated from the Al−V liquid before being poured into the mould, these V-containing phases will have not enough time to transform into others during rapid solidification. These V-containing phases will be remained in the as-cast Al-based Al−V master alloys, which gives the chance to study the existing forms of the phases containing V element at different temperatures.

3.3 Stepwise heating melting experiment results

Figure 6 shows microstructures and phase constitution of Al-based Al−V master alloy produced at 1000 °C by the stepwise heating melting experiment. It can be clearly identified from Fig. 6(a) that three phases with different morphologies are solidified in the Al matrix, which is consistent with the XRD analysis result (Fig. 6(d)) that the as-cast alloy consists of Al_3V, $Al_{10}V$, Al_7V and Al phases. Based on Refs. [20,21], the petal-like phase (Fig. 6(a)) and plate-like phase (Fig. 6(b)) can be identified to be Al_3V and $Al_{10}V$, respectively. Therefore, the needle-like Phase C can be labelled to be Al_7V phase, which is further confirmed by EDS and TEM analysis. As can be seen in Fig. 6(c), the measured Al/V molar ratio (~6.9:1) is quite close to the stoichiometric ratio of Al_7V. Moreover, based on the TEM analysis results shown in Fig. 7, the crystal structure of needle-like Phase B (Fig. 7(a)) is identified to be Al_7V phase according to the TEM diffraction pattern in Fig. 7(b). Therefore, the type of precipitated V-containing phases can be identified according to their morphologies.

Figure 8 shows the microstructures of Al−V master alloys prepared at 800, 900, 1000, 1050, 1100 and 1150 °C by the stepwise heating melting experiment, respectively, indicating the varying fractions of Al_3V, Al_7V and $Al_{10}V$ phases with increasing pouring temperature. Firstly, V-containing phase mainly solidifies in the form of plate-like $Al_{10}V$ phase in the alloys at the pouring temperature below 1000 °C and $Al_{10}V$ phase almost disappears once the temperature is above 1050 °C. Conversely, petal-like Al_3V phase, which is difficult to form in the alloys solidified at temperature below 900 °C (Figs. 8(a) and (b)), becomes the dominant V-containing phase in the alloys prepared at the pouring temperature ≥1050 °C as shown in Figs. 8(d−f). So, the pouring temperature of 1050 °C is the critical temperature of both the disappearance of $Al_{10}V$ and the formation of Al_3V as the dominant phase.

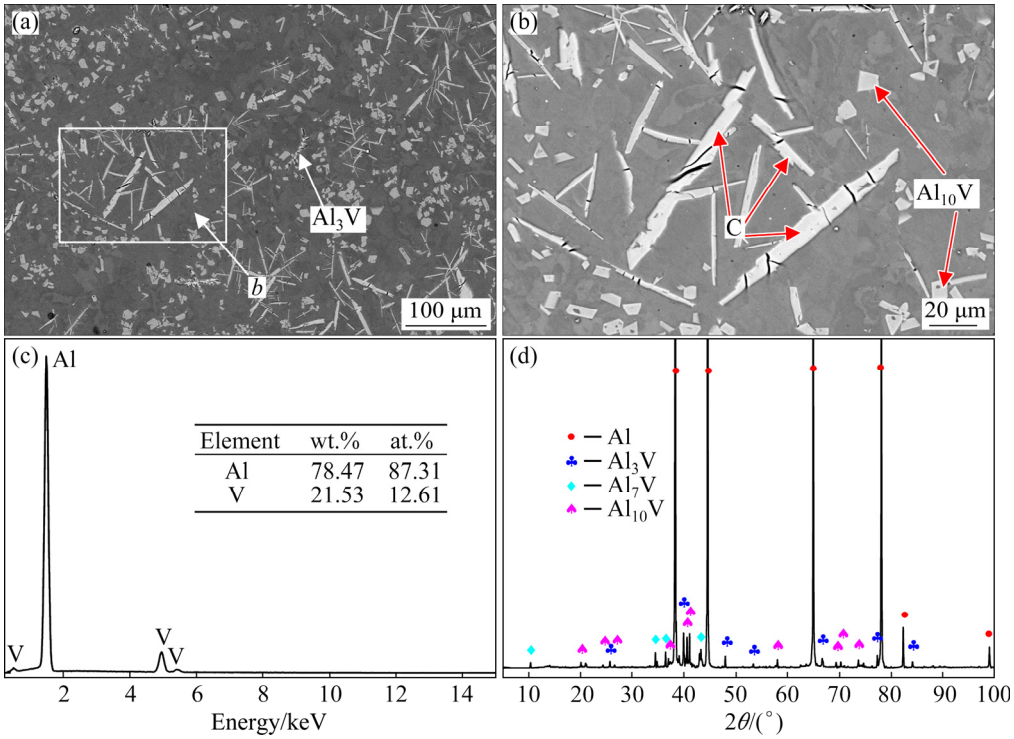

Fig. 6 SEM micrographs, EDS analysis result and XRD pattern of Al-based Al−V master alloy produced at 1000 °C by stepwise heating melting experiment with rapid solidification: (a) SEM image; (b) Magnified image of Area *b* in (a); (c) EDS analysis result of Phase C in (b); (d) XRD pattern of alloy

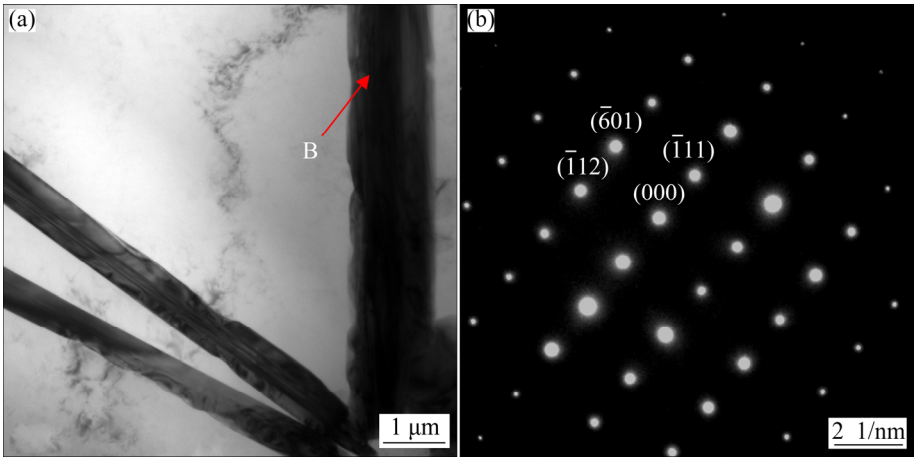

Fig. 7 TEM micrograph of Al-based Al−V master alloy produced at 1000 °C by stepwise heating melting experiment with rapid solidification: (a) Bright field TEM micrograph; (b) Diffraction pattern of Phase B in (a)

Needle-like Al_7V phase was firstly observed in the alloy prepared at 900 °C (Fig. 8(b)). Its fraction increases significantly when the solidification temperature rises to 1000 °C (Fig. 8(c)) and then almost drops to zero at 1050 °C. So, it can be thought that 1000 °C is the critical temperature for the formation of needle-like Al_7V phases with relatively large amounts in the stepwise heating melting experiment.

Table 1 shows the analyzed V contents at the center of the Al−V master alloy ingots prepared at different pouring temperatures in the stepwise heating melting experiment and the corresponding liquidus temperatures of these analyzed V contents according to Al−V binary phase diagram [25,26].

Considering the whole process of the stepwise heating melting experiment, the reason why the actual V content is higher than 4 wt.% at the pouring temperatures of 1050−1150 °C is due to the large reduction of molten Al at the pouring

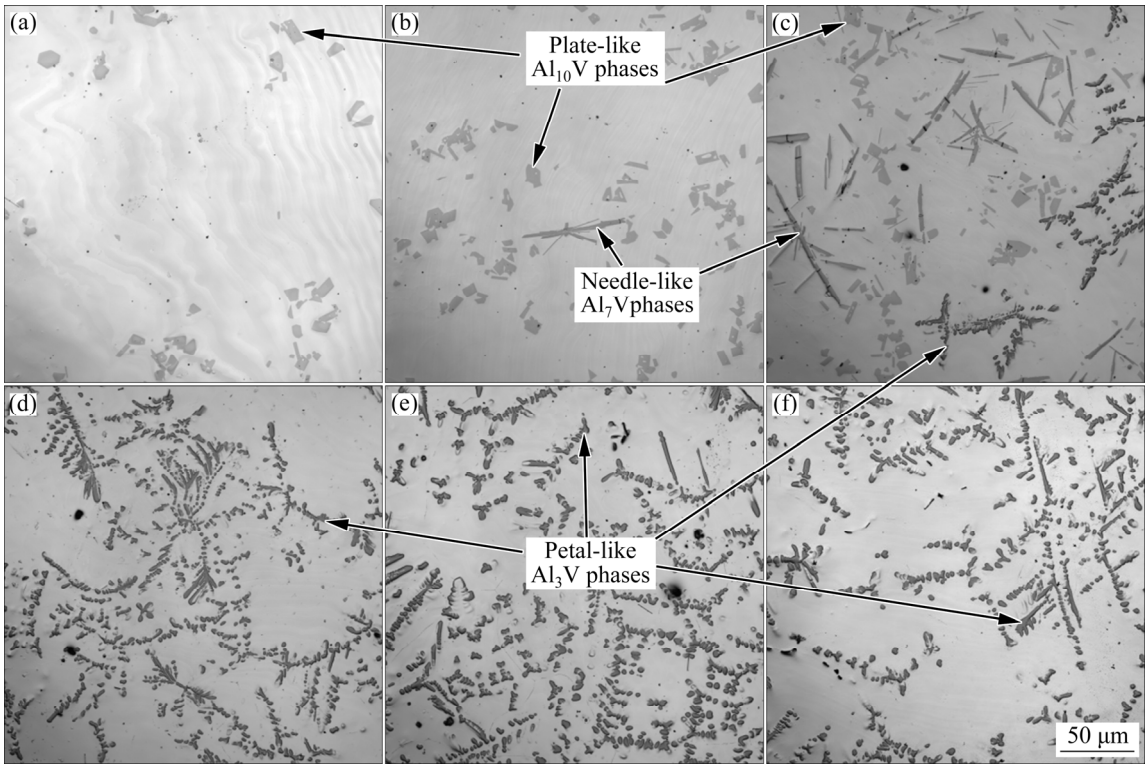

Fig. 8 Microstructures of Al-based Al−V master alloys prepared by stepwise heating melting experiment at different melting temperatures: (a) 800 °C; (b) 900 °C; (c) 1000 °C; (d) 1050 °C; (e) 1100 °C; (f) 1150 °C

Table 1 Analyzed V contents in Al−V master alloys prepared at different pouring temperatures by stepwise heating melting experiment and corresponding liquidus temperatures

Pouring temperature/°C	Analyzed V content/wt.%	Liquidus temperature/°C
800	2.48	974
900	2.65	981
1000	3.06	997
1050	4.18	1035
1100	5.36	1038
1150	5.64	1048

temperatures <1050 °C. It has been reported previously that vanadium does not completely dissolve into the aluminum until the temperature reaches 1100 °C [20]. This indicates that the particles of Al−50wt.%V alloy cannot fully dissolve into the pure Al liquid at the pouring temperatures of 800−1050 °C, so the melt taken out below 1050 °C contains more pure Al liquid (>96 wt.%) and low V content (<4 wt.%). Similarly, the reason why the V content reaches up to 4wt.% at 1050 °C is still not attributed to the complete dissolution of Al−50wt.%V particles into the melt, but more reduction of pure Al liquid in the furnace instead. Further, the Al−50wt.%V particles will dissolve into the pure Al liquid totally with the temperature increasing continuously (1100 and 1150 °C), resulting in that the actual V contents of the remnant Al−V molten liquid in the furnace are much higher than 4 wt.%.

3.4 Stepwise melting cooling experiment results

Figures 9 and 10 show the XRD analysis results and microstructures of Al−V master alloys prepared at 1150, 1100, 1050, 1000, 950 and 830 °C by the stepwise melting cooling experiment, respectively. It can be found from Fig. 9 that there are also three V-containing phases in these alloys: Al_3V, Al_7V and $Al_{10}V$.

Figure 10 shows that the petal-like Al_3V phase dominates in all the alloys except the alloy solidified at 830 °C as it was found in Ref. [20], and this is in accordance with the XRD analysis results shown in Fig. 9. Furthermore, almost all the V-containing phases present in the alloys prepared at above 1050 °C belong to the petal-like Al_3V phases as shown in Figs. 10(a−c). Needle-like Al_7V

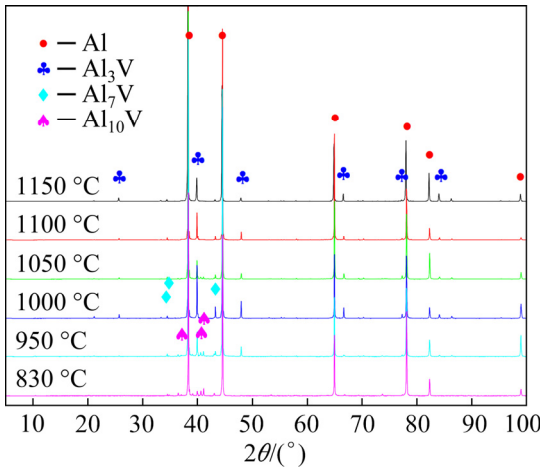

Fig. 9 XRD analysis results of Al−V master alloys prepared at different temperatures by stepwise melting cooling experiment

phases with a relatively large number are present in the alloy prepared at 1000 °C (Fig. 10(d)), but their number reduces obviously when the pouring temperature drops down to 950 °C (Fig. 10(e)) and 830 °C (Fig. 10(f)). Instead, $Al_{10}V$ phase with a plate-like shape starts to be present when the pouring temperature is ≤950 °C, which is in accordance with the results shown in Fig. 9 as well.

Table 2 shows the analyzed V contents at the center of the Al−V master alloys prepared at different pouring temperatures in the stepwise melting cooling experiment and the corresponding liquidus temperatures of these analyzed V contents according to Al−V binary phase diagram [25,26]. From the results in Table 2, it can be concluded that the raw material, i.e. Al−50wt.%V particles, fully dissolves into the pure Al liquid and no V-containing phase is expected to precipitate from the Al−V molten alloy during the holding stage when the pouring temperature is higher than 1000 °C.

It can be also noticed that although all the raw Al−50wt.%V alloy has dissolved into pure Al liquid, the lower the pouring temperature is, the lower the V content is when the temperature is ≤1000 °C. In addition, it is interested that the pouring temperatures (1000, 950 and 830 °C) are lower than the corresponding liquidus temperatures of the analyzed V contents (1017, 993 and 971 °C), according to Al−V binary phase diagram. This can be understood on the other hand that, the remnant Al−V liquid is supersaturated before it is poured at 1000, 950 and 830 °C, which should be due to the higher temperature dropping rate during the melting process, compared to that in the Al−V binary equilibrium phase diagram.

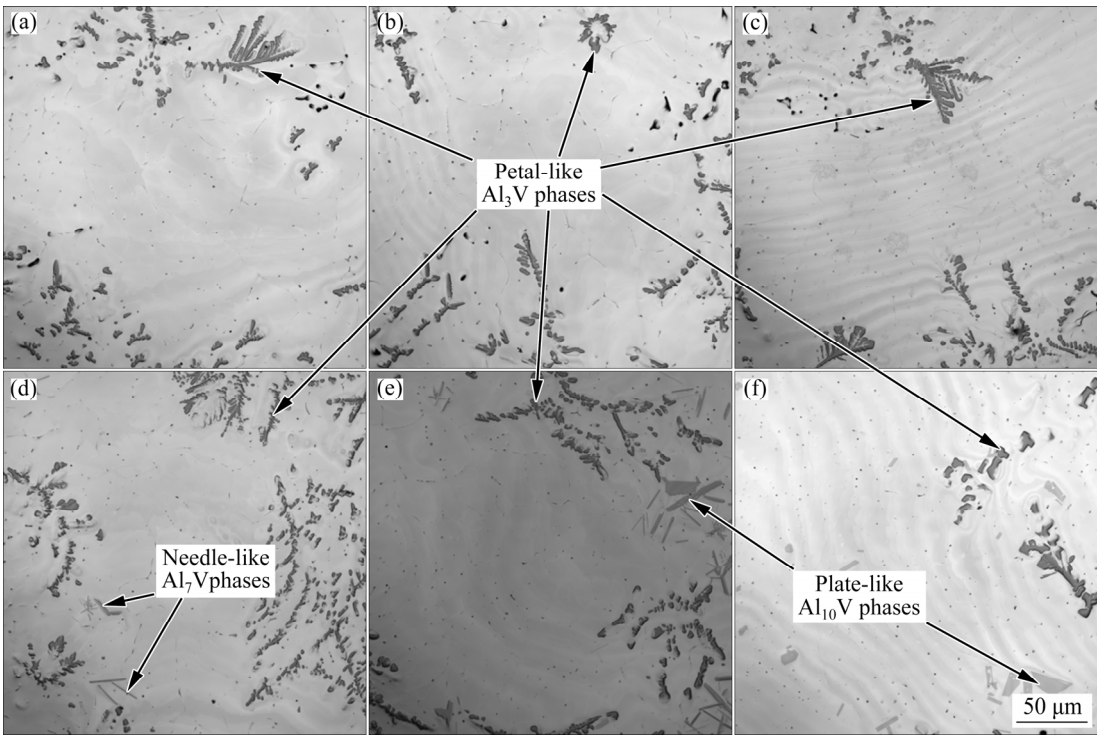

Fig. 10 Microstructures of Al-based Al−V master alloys prepared by stepwise melting cooling experiment at different pouring temperatures: (a) 1150 °C; (b) 1100 °C; (c) 1050 °C; (d) 1000 °C; (e) 950 °C; (f) 830 °C

Table 2 Analyzed V contents in Al−V master alloys prepared at different pouring temperatures by stepwise melting cooling experiment and corresponding liquidus temperatures

Pouring temperature/°C	Analyzed V content/wt.%	Liquidus temperature/°C
1150	4.08	1030
1100	4.02	1029
1050	3.98	1027
1000	3.68	1017
950	2.96	993
830	2.43	971
730	2.39	969

Moreover, at the end of the stepwise melting cooling experiment, the remnant Al−V alloy molten at the bottom of graphite crucible was poured into the water-cooled copper mould at 730 °C. The V content of this ingot was measured to be 2.39 wt.%, which is quite close to that of the alloy at the pouring temperature of 830 °C. Microstructural analysis (Fig. 11) shows the formation of Al_3V phases (large particle) and $Al_{10}V$ phases (fine particle), with the area fractions being about 6.05% and 1.53%, respectively. It is interested that the fraction of Al_3V phases increases significantly in the ingot in Fig. 11, instead of the continuous decline of Al_3V phase content with the decrease of pouring temperature shown in Fig. 10.

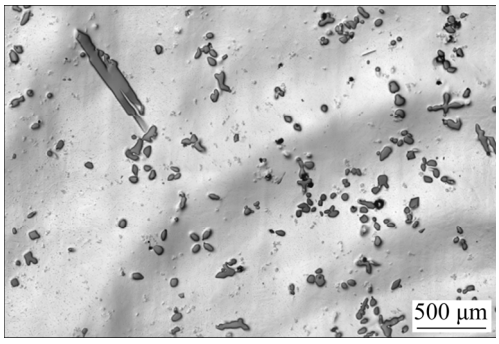

Fig. 11 Microstructure of ingot produced by remnant molten alloy at 730 °C at end of stepwise melting cooling experiment

Considering the process of the stepwise melting cooling experiment, the reason should be that some V-containing phases pre-precipitate from the Al−V liquid in the graphite crucible due to the low temperature (≤1000 °C) at first, and then some of them would settle to the bottom of the crucible due to their higher density, compared to the density of the Al−V liquid. As a result, not only the actual V content of the Al−V liquid which is taken out of the graphite crucible and then poured into the mould at ≤1000 °C is lower than 4 wt.%, but also the Al_3V phase content increases in the ingot produced by the remnant Al−V melt at 730 °C.

In addition, it can be found from Fig. 11 that the size of Al_3V phase is quite larger than those shown in Fig. 10. The time spent on the temperature dropping from 1000 to 730 °C is obviously longer than that from 1150 to 1000 °C due to the temperature gradient, so the combination effects of the long time and the high temperature (730−1000 °C) result in the growth of pre-precipitated Al_3V phases in the Al−V molten alloy. What is more, it can be summarized that the V-containing phases which are formed by the pre-precipitation from the Al−V liquid below 1000 °C and consequently lead to the decrease of V content of the Al−V master alloy are mainly Al_3V phases.

4 Discussion

It is well known that Al_3V phase and $Al_{10}V$ phase are usually present in the Al−4wt.%V alloys prepared under different conditions [20,22]. Al_3V phase with the petal-like shape is good for Al−4wt.%V master alloy because it will improve the microstructure and mechanical properties of aluminum alloys, while the plate-like $Al_{10}V$ phase is harmful due to its shape feature and obvious structure heredity [22]. However, their evolution and transformation process are not discussed clearly. With the help of the stepwise heating melting experiment and stepwise melting cooling experiment, V-containing phases evolution was investigated in detail.

Figure 12 shows the dependence of the area fractions of petal-like Al_3V phase, needle-like Al_7V phase and plate-like $Al_{10}V$ phase on the pouring temperatures in different experiments based on Figs. 8 and 10. In the stepwise heating melting experiment (Fig. 12(a)), with the increase of the pouring temperature, the area fraction of $Al_{10}V$ phase increases and then decreases, with the maximum area fraction being 15.97% at 900 °C. Al_7V phase presents a similar trend, with the maximum area fraction being 3.12% at 1000 °C.

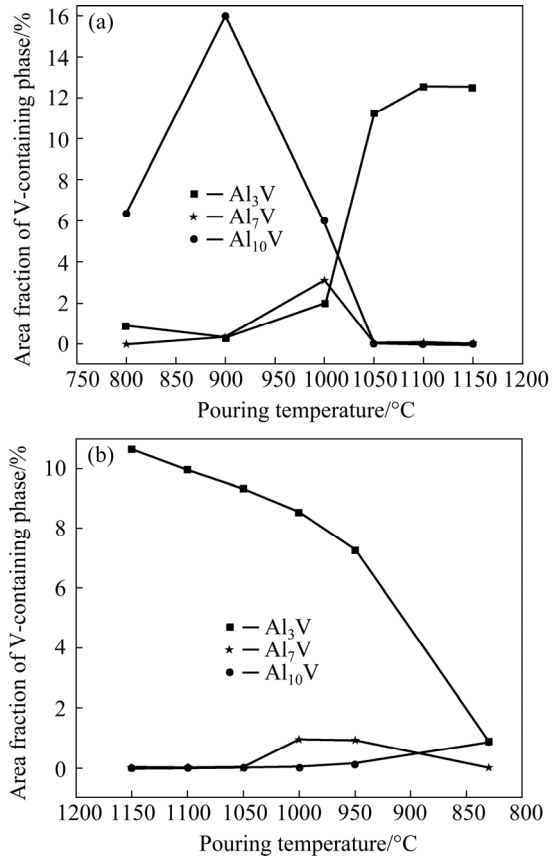

Fig. 12 Dependence of area fractions of Al_3V, Al_7V and $Al_{10}V$ phases in as-cast Al−V master alloys prepared by stepwise heating melting experiment (a) and stepwise melting cooling experiment (b) on different pouring temperatures

While, the number of Al_3V phase increases continuously with the increase of pouring temperature from 800 to 1150 °C.

In the stepwise melting cooling experiment (Fig. 12(b)), with the pouring temperature dropping, the number of $Al_{10}V$ phase increases slightly, while that of Al_3V phase decreases dramatically. The number of Al_7V phase increases to the maximum (0.94%) firstly at 1000 °C and then decreases, which is in accordance with the change in the stepwise heating melting experiment.

4.1 Evolution of Al_3V phase and Al_8V_5 phase (matrix) in raw Al−50wt.%V alloy

Al_3V phase presents a distinct needle-like morphology in the Al−50wt.%V raw material (Figs. 2 and 4) and always presents a petal-like morphology instead in all the Al-based Al−V mater alloys solidified in the copper mould. This indicates the occurrence of the phase transformation of needle-like Al_3V phase at the time of the raw material being added into pure Al liquid at 800−1150 °C. Whether needle-like Al_3V phase transforms into Al_7V phase or dissolves into Al melt depends on the holding temperature and the corresponding liquidus temperature. Meanwhile, the matrix phase, Al_8V_5, will transform into Al_3V phase based on the Al−V binary phase diagram [25,26], with the observation of none of needle-like Al_3V phase but petal-like Al_3V phase instead.

4.2 Evolution of V-containing phases in stepwise heating melting experiment

4.2.1 At pouring temperatures ≤1000 °C

Based on Table 1, the pouring temperatures of Al−V alloys (≤1000 °C) are lower than the corresponding liquidus temperatures (974, 981 and 997 °C). So, the needle-like Al_3V phases existing in the Al−50wt.%V particles (Figs. 2 and 4) cannot fully dissolve into the molten Al alloy in the melting process at pouring temperatures ≤1000 °C. It should be expected that the needle-like Al_3V phase suspended in molten Al alloy will transform into Al_7V phase during the melting process based on Al−V binary phase diagram [25], which is consistent with the observation that Al_7V phase also appears as needle shape. Its largest area fraction (3.12% in Fig. 12(a)) is present at the pouring temperature of 1000 °C (Fig. 8(c)), so the needle-like Al_7V phase, as a kind of metastable phase, has the highest stability at 1000 °C. Almost all the Al_7V phases will keep on changing into plate-like $Al_{10}V$ phase at temperatures <1000 °C, as shown in Figs. 8(a) and (b). Although the stability of Al_7V phase is the highest at 1000 °C, its stability should be still lower than that of Al_3V phase and $Al_{10}V$ phase with the area fractions being 1.96% and 5.99%, respectively, as shown in Fig. 8(c) and Fig. 12(a).

In addition, Al−V alloys prepared at the pouring temperatures of 800 and 900 °C also contain low fractions of petal-like Al_3V phases, with the values being 0.88% and 0.26%, respectively, as shown in Figs. 8(a), (b) and Fig. 12(a). Here, petal-like Al_3V phases can be formed in two paths: (1) They are transformed from the matrix phases (Al_8V_5 phases) of the Al−50wt.%V alloy during melting based on the Al−V binary phase diagram and then retained in the

as-cast ingots in the rapid solidification; (2) They are directly formed by precipitation from the molten Al−V alloy in the rapid solidification. Therefore, the evolution process of V-containing phases during the preparation of Al−V master alloys at the pouring temperatures ≤1000 °C can be described by Steps (1)−(3) in Fig. 13.

Step (1) shows the main evolution of plate-like $Al_{10}V$ phases and the formation of petal-like Al_3V phases can be illustrated by Steps (2) and (3) in the Al−V master alloys prepared at temperatures less than 1000 °C (Figs. 8(a) and (b)). Similarly, V-containing phases evolution in the Al−V master alloy prepared at 1000 °C can be described by Steps (1) and (2), resulting in the co-existence of needle-like Al_7V phases, plate-like $Al_{10}V$ phases and petal-like Al_3V phases.

4.2.2 At pouring temperature of 1050 °C

Almost all the needle-like Al_3V phases in the raw Al−50wt.%V alloy should dissolve into pure Al liquid as only petal-like Al_3V phases are present in Fig. 8(d). Al_8V_5 phases (matrix) should transform into petal-like Al_3V phases firstly during melting, and then some Al_3V phases should dissolve into the molten Al but others should still co-exist with Al−V liquid, which is similar to the evolution of Al_8V_5 phase in Section 4.2.1. As a result, a great number of petal-like Al_3V phases will precipitate from Al−V molten alloy during rapid solidification [20,21] and the Al_3V phases which co-exist with the Al−V liquid are finally retained in the alloy ingots. The evolution process of V-containing phase in the alloy prepared at 1050 °C can be described by Steps (2) and (3).

4.2.3 At pouring temperatures ≥1100 °C

When the temperatures continuously increase to 1100 and 1150 °C, the main V-containing phases are still petal-like Al_3Vphases (Figs. 8(e) and (f)) and V contents are much larger than 4 wt.% (Table 1). Therefore, both the needle-like Al_3V phases in raw material and the petal-like Al_3V phases which are firstly transformed from Al_8V_5 phases (matrix) should dissolve into Al liquid totally during melting, leading to the precipitation of a great number of petal-like Al_3V phases during rapid solidification. The evolution process of V-containing phase in these alloys prepared at temperatures ≥1100 °C can be described by Step (3) in Fig. 13 and Step (4) in Fig. 14.

4.3 Evolution of V-containing phases in stepwise melting cooling experiment

4.3.1 At pouring temperatures >1000 °C

Since the raw material was firstly held at

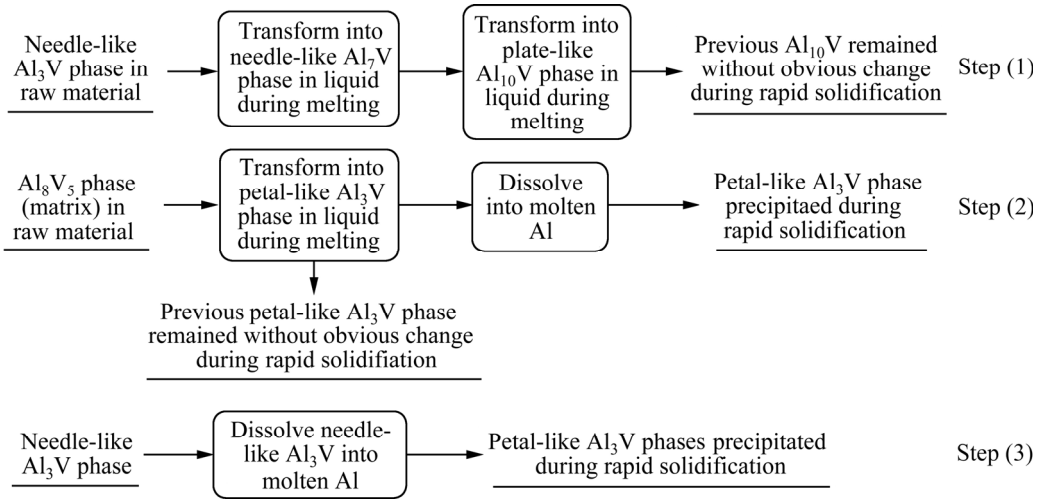

Fig. 13 Evolution process of V-containing phases during preparation of Al−V master alloys at pouring temperatures ≤1000 °C in stepwise heating melting experiment

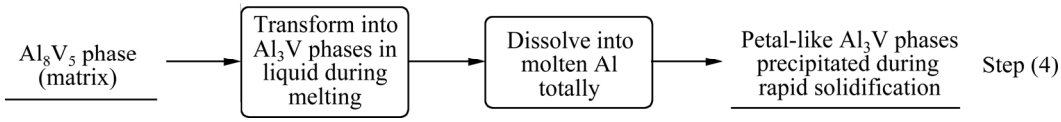

Fig. 14 Evolution process of Al_8V_5 phases during preparation of Al−V master alloys at pouring temperatures ≥1100 °C in stepwise heating melting experiment

1150 °C, with the V content being about 4 wt.% (Table 2), it could be thought that the raw Al−50wt.%V alloy must have dissolved into the Al molten totally before stepwise cooling starts, and then precipitated in the form of petal-like Al_3V phases during rapid solidification, with the area fractions of 10.64% (1150 °C), 9.95% (1100 °C) and 9.33% (1050 °C) respectively, as shown in Fig. 12(b). Therefore, the evolution process of V-containing phases during the preparation of the Al−V alloys at the pouring temperatures >1000 °C can be described by Step (3) (Fig. 13) and Step (4) (Fig. 14).

4.3.2 At pouring temperatures ≤1000 °C

When the temperature reduces to 1000 °C, some Al_3V phases will precipitate from the Al−V melt before being poured into the water-cooled copper mould. It is also an accumulating process as the pouring temperature decreases form 1000 °C. However, Figs. 10(d) and (e) show that the number of petal-like Al_3V phases in the alloys prepared at the pouring temperatures of 1000 and 950 °C does not decrease largely (area fractions of 8.53% and 7.23%, respectively in Fig. 12(b)), so there is no doubt that most of petal-like Al_3V phases in these alloys are precipitated from Al−V melt during rapid solidification.

Figure 10 also shows that the number of needle-like Al_7V phase is larger (Fig. 12(b)) when the pouring temperature is 1000 °C, which is in accordance with the regularity obtained by the stepwise heating melting experiment. And the area fractions of plate-like $Al_{10}V$ phase increase to 0.1% and 0.88% (Fig. 12(b)) in the alloys prepared at the pouring temperatures of 950 and 830 °C, respectively. Therefore, according to Al−V binary phase diagram [25,26] and the quantity changes of V-containing phases with pouring temperature in Fig. 12(b), it can be concluded that once the Al_3V phases are precipitated from the Al−V molten alloy at the temperatures ≤1000 °C during melting, some of them will transform into needle-like Al_7V phases. The number of Al_7V phases increases with the pouring temperature dropping, and reaches the maximum at 1000 °C due to the large stability of the Al_7V phase at this moment. When the temperature continues to drop down to <1000 °C, some needle-like Al_7V phases will further transform into plate-like $Al_{10}V$ phases during melting as shown in Figs. 10(e) and (f). The number of $Al_{10}V$ phases increases, but V content in the Al−V molten alloy decreases with the drop of the pouring temperature (<1000 °C). So, it can be inferred that the combined effects of the lower V content (<3 wt.%) in Al−V molten alloy and lower temperature (<1000 °C) should promote the transformation of $Al_{10}V$ phase from Al_7V phase during melting. The evolution process of V-containing phase during the preparation of the Al−V alloys prepared at the pouring temperatures ≤1000 °C can be described by Step (5) in Fig. 15.

4.4 Overall evolution process of V-containing phases

According to the Steps (1)−(5) in Figs. 13−15, the whole evolution process of V-containing phases during the preparation of Al-based Al−V master alloys at temperatures of 800−1150 °C can

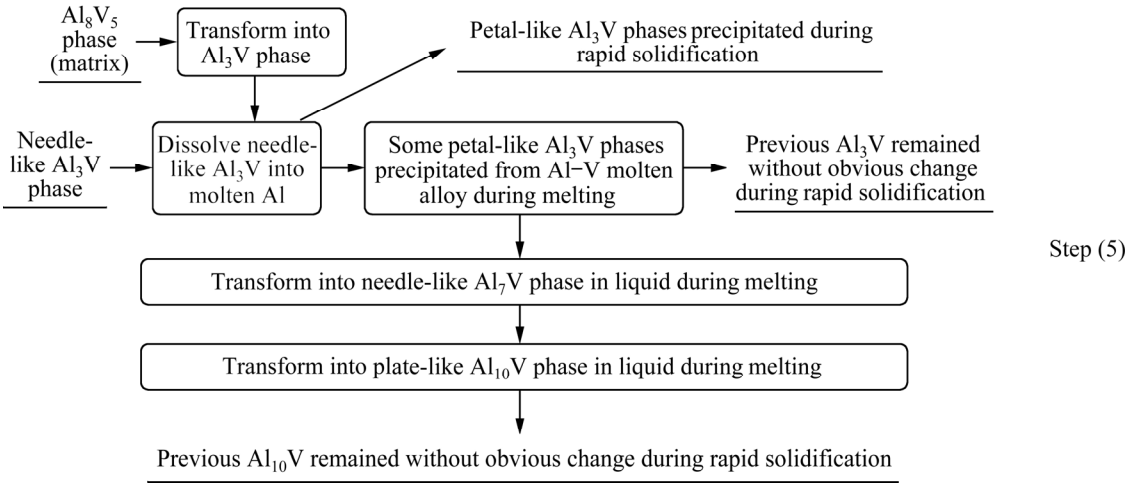

Fig. 15 Evolution process of V-containing phases during preparation of Al−V master alloys at pouring temperatures ≤1000 °C in stepwise melting cooling experiment

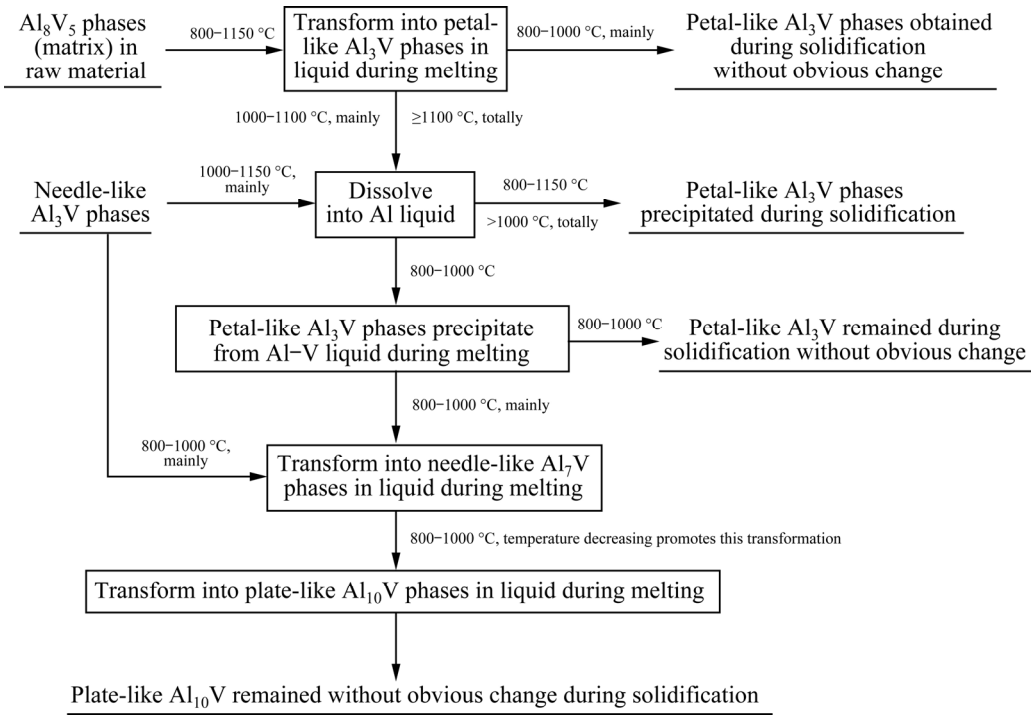

Fig. 16 Overall evolution process of V-containing phases during preparation of Al-based Al−V master alloys at pouring temperatures of 800−1150 °C

be summarized in Fig. 16, where "mainly" and "totally" mean that the V-containing phase evolution will occur mainly and totally in this way, respectively.

5 Conclusions

(1) Needle-like Al_3V phase and Al_8V_5 phases as the matrix are present in the raw material (Al−50wt.%V alloy), but three V-phases: petal-like Al_3V phase, needle-like Al_7V phase and plate-like $Al_{10}V$ phase are present in the Al-based Al−V master alloys.

(2) Needle-like Al_7V phase, as a metastable phase, is transformed from Al_3V phase at the temperatures ≤1000 °C during melting and has the highest stability at 1000 °C. The maximum area fractions of Al_7V phases obtained by heating and cooling experiments are 3.12% and 0.94% respectively. $Al_{10}V$ phase, whose area fraction increases with the drop of the temperature, is evolved from Al_7V phase during melting.

(3) Petal-like Al_3V phases can be formed by three ways: transformed from Al_8V_5 in raw material during melting, pre-precipitated from Al−V molten alloy during melting and precipitated during rapid solidification. With the increase of temperature, the number of Al_3V phases formed during rapid solidification at 800−1150 °C increases, but it decreases instead for Al_3V phases precipitated from Al−V molten alloy during melting at 800−1000 °C.

Acknowledgments

This work was financially supported by the National Natural Science Foundation of China (No. 51804010), the 2020 Yuyou Talent Training Plan Project of North China University of Technology, China (No. 214051360020XN212/014), and the R&D Program of Beijing Municipal Education Commission, China (No. KM201910009007).

References

[1] LOHAR A K, MONDAL B, RAFAJA D, KLEMM V, PANIGRAHI S C. Microstructural investigations on as-cast and annealed Al−Sc and Al−Sc−Zr alloys [J]. Materials Characterization, 2009, 60: 1387−1394.

[2] ZHANG Wei, XING Yuan, JIA Zhi-hong, YANG Xiao-fang, LIU Qing, ZHU Chang-long. Effect of minor Sc and Zr addition on microstructure and properties of ultra-high strength aluminum alloy [J]. Transactions of Nonferrous Metals Society of China, 2014, 24: 3866−3871.

[3] CASARI D, LUDWIG T H, MERLIN M, ARNBERG L, GARAGNANI G L. The effect of Ni and V trace elements

on the mechanical properties of A356 aluminium foundry alloy in as-cast and T6 heat treated conditions [J]. Materials Science and Engineering A, 2014, 610: 414−426.

[4] GIOVANNIM D T, TERESA M, CERRI E, CASARI D, MERLIN M, ARNBERG L, GARAGNANI G L. The influence of Ni and V trace elements on high temperature tensile properties and aging of A356 aluminum foundry alloy [J]. Metallurgical and Materials Transactions A, 2016, 47: 2049−2057.

[5] WU Yu-na, LIAO Heng-cheng, ZHOU Ke-xin. Effect of minor addition of vanadium on mechanical properties and microstructures of as-extruded near eutectic Al−Si−Mg alloy [J]. Materials Science and Engineering A, 2014, 602: 41−48.

[6] SHAHA S K, CZERWINSKI F, KASPRZAK W, FRIEDMAN J, CHEN D L. Effect of Cr, Ti, V, and Zr micro-additions on microstructure and mechanical properties of the Al−Si−Cu−Mg cast alloy [J]. Metallurgical and Materials Transactions A, 2016, 47: 2396−2409.

[7] RAKHMONOV J, TIMELLI G, BONOLLO F. Characterization of the solidification path and microstructure of secondary Al−7Si−3Cu−0.3Mg alloy with Zr, V and Ni additions [J]. Materials Characterization, 2017, 128: 100−108.

[8] ERDENIZ D, NASIM W, MALIK J, YOST A R, PARK S, LUCA A D, VO N Q, KARAMAN I, MANSOOR B, SEIDMAN D N, DUNAND D C. Effect of vanadium micro-alloying on the microstructural evolution and creep behavior of Al−Er−Sc−Zr−Si alloys [J]. Acta Materialia, 2017, 124: 501−512.

[9] ELHADARI H A, PATEL H A, CHEN D L, KASPRZAK W. Tensile and fatigue properties of a cast aluminum alloy with Ti, Zr and V additions [J]. Materials Science and Engineering A, 2011, 528: 8128−8138.

[10] KHALIQ A, ALI H T, YUSUF M. Thermodynamic and kinetic analysis of CrB_2 and VB_2 formation in molten Al−Cr−V−B alloy [J]. Transactions of Nonferrous Metals Society of China, 2021, 31: 3162−3176.

[11] DING Wan-wu, XIA Tian-dong, ZHAO Wen-jun. Performance comparison of Al−Ti master alloys with different microstructures in grain refinement of commercial purity aluminum [J]. Materials, 2014, 7: 3663−3676.

[12] HOSSEINPOURI M, MIRMONSEF S A, SOLTANIEH M. Production of Al−Ti master alloy by aluminothermic reduction technique [J]. Canadian Metallurgical Quarterly, 2007, 46: 139−143.

[13] YANG Qing-bo, DENG Yan-jun, YANG Mou, ZHANG Zhi-qing, LI Wei-guo, LIU Qing. Effect of Al_3Zr particles on hot-compression behavior and processing map for Al−Cu−Li based alloys at elevated temperatures [J]. Transactions of Nonferrous Metals Society of China, 2020, 30: 872−882.

[14] MOHAMMADI A, ENIKEEV N A, MURASHKIN M Y, ARITA M, EDALATI K. Developing age-hardenable Al−Zr alloy by ultra-severe plastic deformation: Significance of supersaturation, segregation and precipitation on hardening and electrical conductivity [J]. Acta Materialia, 2021, 203: 503−507.

[15] JUNG J G, CHO Y H, KIM S D, KIM S B, LEE S H, SONG K, EUH K, LEE J M. Mechanism of ultrasound-induced microstructure modification in Al−Zr alloys [J]. Acta Materialia, 2020, 199: 73−84.

[16] FANG Ling, ZHANG Zhuo, FANG Hua-chan, HUANG Lan-ping, CHEN Kang-hua. Effects of Si additions on the precipitation evolution of dilute Al−Zr−Yb alloys [J]. Materials Characterization, 2019, 152: 130−133.

[17] ZUO Min, JIANG Kun, LIU Xiang-fa. Refinement of hypereutectic Al−Si alloy by a new Al−Zr−P master alloy [J]. Journal of Alloys and Compounds, 2010, 503: 26−30.

[18] ZHANG Li-li, JIANG Hong-xiang, HE Jie, ZHAO Jiu-zhou. Kinetic behaviour of TiB_2 particles in Al melt and their effect on grain refinement of aluminium alloys [J]. Transactions of Nonferrous Metals Society of China, 2020, 30: 2035−2044.

[19] XU Cong, DU Rou, WANG Xue-jiao, HANADA S, YAMAGATA H, WANG Wen-hong, MA Chao-li. Effect of cooling rate on morphology of primary particles in Al−Sc−Zr master alloy [J]. Transactions of Nonferrous Metals Society of China, 2014, 24: 2420−2426.

[20] MENG Yi, CUI Jian-zhong, ZHAO Zhi-hao, ZUO Yu-bo. Study on microstructures of Al−4wt.%V master alloys [J]. Metallurgical and Materials Transactions A, 2014, 45: 3741−3747.

[21] ZHU Qing-feng, MENG Yi, KANG Yan-lei, KONG Shu-ping, OU Yang-peng, ZUO Yu-bo. Effect of cooling rate on morphology and type of vanadium-containing phases in Al−10V master alloy [J]. China Foundry, 2019, 16(5): 300−306.

[22] MENG Yi, CUI Jian-zhong, ZHAO Zhi-hao, ZUO Yu-bo. Effect of vanadium on the microstructures and mechanical properties of an Al−Mg−Si−Cu−Cr−Ti alloy of 6xxx series [J]. Journal of Alloys and Compounds, 2013, 573: 102−111.

[23] LAI J, SHI C J, CHEN X G. Effect of V addition on recrystallization resistance of 7150 aluminum alloy after simulative hot deformation [J]. Materials Characterization, 2014, 96: 126−134.

[24] SHI C J, CHEN X G. Evolution of activation energies for hot deformation of 7150 aluminum alloys with various Zr and V additions [J]. Materials Science and Engineering A, 2016, 650: 197−209.

[25] MURRAY J L. Al−V (aluminum−vanadium) [J]. Bulletin of Alloy Phase Diagrams, 1989, 10: 351−357.

[26] OKAMOTO H. Al−V (aluminum−vanadium) [J]. Journal of Phase Equilibria and Diffusion, 2012, 33: 491.

Al 基 Al−V 中间合金制备过程中含 V 相的演变

蒙 毅[1]，杨 越[1]，李 岑[1]，曹雷刚[1]，赵志浩[2]，朱庆丰[2,3]，崔建忠[3]

1. 北方工业大学 机械与材料工程学院，北京 100144；
2. 东北大学 材料科学与工程学院，沈阳 110004；
3. 东北大学 材料电磁过程研究教育部重点实验室，沈阳 110004

摘 要：由于熔炼和凝固过程显著影响含 V 相的结构演变，而不同含 V 相后续又会影响工业铝合金和钛合金的组织和性能，因此，本文作者基于升温熔炼和降温熔炼实验，结合快速凝固制备 Al 基 Al−V 中间合金，研究不同 Al−V 合金中含 V 相的相变规律。研究结果表明，Al−50wt.%V 合金原料由针状 Al_3V 相和 Al_8V_5 基体相组成，而后续制备所得的 Al−V 中间合金由花瓣状 Al_3V 相、针状 Al_7V 相和片状 $Al_{10}V$ 相构成。由 Al_3V 相转变而来的针状亚稳 Al_7V 相将进一步转变为片状 $Al_{10}V$ 相。$Al_{10}V$ 相数量随熔炼温度(800~1000 °C)的降低而增大。花瓣状 Al_3V 相可由 Al_8V_5 相转变而来，在熔炼过程中从 Al−V 熔体中预析出以及在合金凝固过程中析出形成。

关键词：Al 基 Al−V 中间合金；相变；含 V 相；快速凝固；浇铸温度

(Edited by Wei-ping CHEN)